02,10

Magnetic properties of the superconducting Ga−In−Sn alloy under nanoconfinement

© M.V. Likholetova[1], E.V. Charnaya[1,¶], O.D. Shevtsova[1], Yu.A. Kumzerov[2], A.V. Fokin[2]

[1] St. Petersburg State University,
St. Petersburg, Russia
[2] Ioffe Institute,
St. Petersburg, Russia

¶ E-mail: e.charnaya@spbu.ru

Received September 5, 2024
Revised September 7, 2024
Accepted September 8, 2024

Triple alloy of gallium, indium, and tin is considered as a prospective material for designing self-healing superconducting micro- and nanoelements. In the present work we carried out studies of (dc) magnetization for the Ga−In−Sn alloy nanostructured due to embedding into a nanoporous silica matrix within the temperature range 1.8−10 K and magnetic fields up to 70 kOe. The alloy composition was close to the eutectic point. Three superconducting transitions were revealed with temperatures 6.24, 5.58 and 3.24 K. Weak superconductivity was observed below 7 K. The transitions were attributed to segregates formed within pores. Magnetic instabilities were found in isotherms of magnetization. Phase diagrams were constructed, and the character of the critical lines was discussed.

Keywords: eutectic Ga−In−Sn alloy, nanoconfinement, superconductivity, dc magnetization.

DOI: 10.61011/PSS.2024.10.59618.231

1. Introduction

Nanostructured superconductors are promising materials in micro- and nanoelectronics, robotics and information technology because of their unique properties [1]. Various types of nanosuperconductors are actively studied: from isolated nanoparticles to three-dimensional nanocomposites [2]. Special attention is paid to the study of the superconductivity of metals and metallic alloys introduced into nanoporous matrices with different pore network geometries. Silicate porous glasses, zeolites, opals and porous ceramics are used as matrices. Thus, it is possible to create nanocomposites of various morphologies with a certain size and shape of superconducting inclusions, as well as to control their mutual location and connectivity. Recent studies have shown that the superconducting properties of metals and alloys in nanoconfinement significantly differ from the superconducting properties of the corresponding bulk materials [2–4].

Gallium-containing alloys are particularly distinguished among metallic alloys. They are non-toxic, highly conductive and withstand large mechanical deformations [5], and they also have low melting points. These characteristics ensure the use of gallium-containing alloys in soft robotics, flexible electronics, sensors, etc. [6]. In addition, they are considered for use as superconducting contacts with the ability to self-heal when heated to room temperature [7]. Such contacts can increase the durability of many nanoelectronic devices.

A triple alloy of gallium, indium and tin is one of the most promising superconducting alloys containing gallium. Some studies of the superconductivity of this alloy were carried out earlier. Ga−In−Sn bulk alloy with a composition close to eutectic was studied in Ref. [8] and a superconducting transition was detected at a temperature of 6 K. The superconductivity of nanodroplets of Ga−In−Sn with an average diameter of 110 nm and with a different ratio of components in the alloy was studied in Ref. [9]. The maximum critical temperature obtained was 6.6 K. Superconducting transition in nanoparticles of Ga−In−Sn alloy with a diameter of 500 nm was observed at a temperature of 6.28 K [10]. The effect of nanoconfinement on the superconductivity of Ga−In−Sn alloy of the eutectic composition was studied in Ref. [11]. The temperature dependences of the ac magnetization of the alloy introduced into porous silicate glass were measured when various bias fields were applied. Two superconducting transitions were detected at temperatures of 5.6 and 3.1 K. In addition, the dynamics of superconducting vortices was studied and the thermal activation character of their motion was proved. This paper provides the results of studies of dc magnetization for the same nanocomposite conducted for obtaining more detailed information about the superconductivity of Ga−In−Sn triple alloy in nanoconfinement.

2. Sample and experiment

The silicate porous matrix was obtained from two-phase sodium borosilicate glass by acid leaching. The average pore size was 7 nm according to nitrogen porosimetry. Ga−In−Sn alloy was introduced into the matrix in the

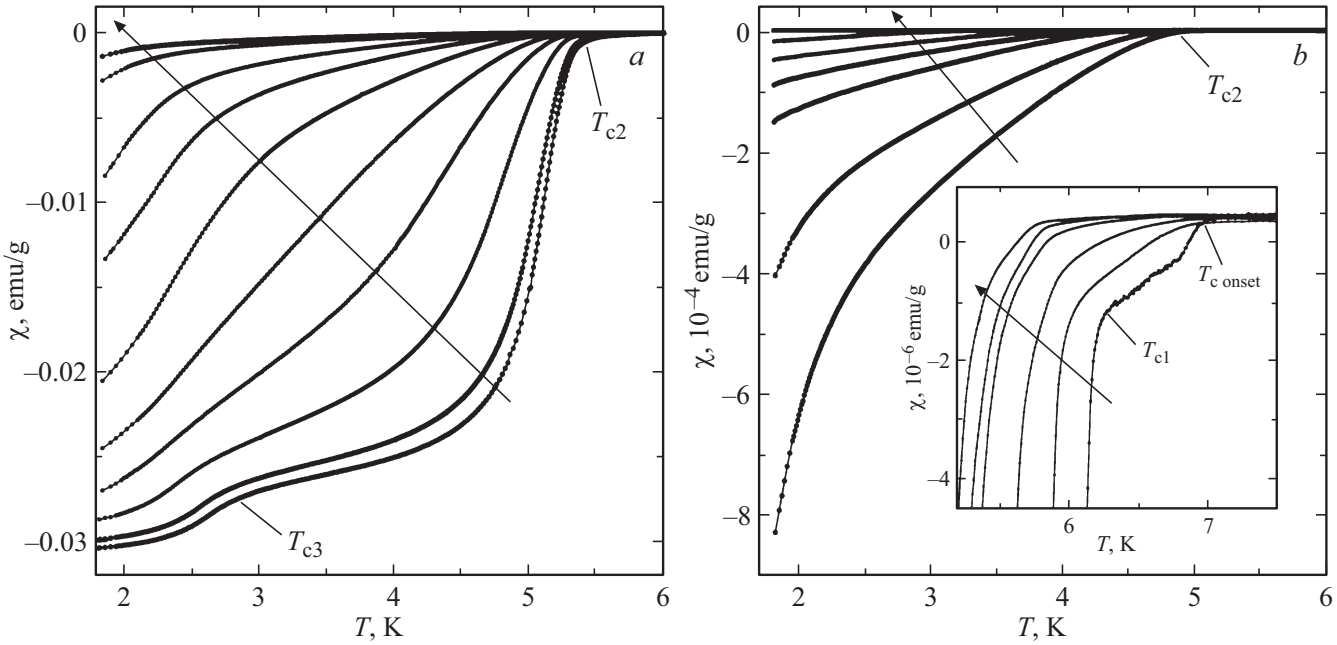

Figure 1. Temperature dependences of *dc*-susceptibility obtained in the ZFC mode in different magnetic fields: *a* — 5, 7, 20, 50, 100, 200, 300, 500, 1000, 1500 Oe; *b* — 2, 3, 5, 7, 10, 15, 20, 30, 40 kOe. The insert shows the dependencies $\chi(T)$ for magnetic fields of 7, 50, 100, 200, 300, 500 Oe on an enlarged scale in the region of the onset of the transition to a superconducting state. The arrows indicate the direction of increase of the magnetic field.

molten state under high pressure up to 10 kbar. The composition of the alloy was close to the eutectic point (77.2 at.% Ga, 14.4 at.% In and 8.4 at.% Sn [12]). The pore filling factor of the matrix was calculated by the weight of the empty and filled glass matrix and was approximately 80%. A plate was cut out of the obtained nanocomposite, the surface of which was carefully cleaned of traces of a bulk alloy. The sample mass m was 33.21 mg.

The dc magnetization M was measured using SQUID magnetometer MPMS 3 manufactured by Quantum Design in the temperature range from 1.8 to 10 K. The temperature dependences of magnetization were obtained in the heating mode in a magnetic field after pre-cooling in a zero field (zero-field cooled, ZFC) and in the subsequent cooling mode in a magnetic field (field-cooled-cooling, FCC) with the application of permanent magnetic fields H from 1 Oe up to 70 kOe. The field dependences of magnetization were measured at a constant temperature in the range of magnetic fields from −70 to 70 kOe.

The specific *dc*-magnetization was calculated as $M = \mu/m$, where μ is the experimentally obtained magnetic moment of the sample. The specific *dc*-susceptibility was calculated as $\chi = M/H$.

3. Results

The temperature dependences of ZFC susceptibility for various magnetic fields are shown in Figures 1 and 2. The transition to the superconducting state is carried out in several stages at critical temperatures T_{c1}, T_{c2} and T_{c3}. Superconducting transitions are smeared. Critical temperatures decrease with an increase of the magnetic field and the smearing of superconducting transitions increases. The first and second transitions are observed above 1.8 K in magnetic fields up to 30 and 20 kOe, respectively, and the third transition is shifted below the limit of the operating range of the magnetometer in magnetic fields stronger than 100 Oe. The critical temperatures for various fields were determined using the first temperature derivative of susceptibility due to the smearing of transitions. T_{c1} was calculated as the temperature at which the first sharp deviation of the derivative from the horizontal line occurred, T_{c2} was calculated as the temperature at which the derivative was 1.5% of its maximum value, T_{c3} was determined as the temperature at which the first derivative increased by 0.1% below the local minimum immediately above the third transition as the temperature decreased. Critical temperatures $T_{c1} = 6.24$ K, $T_{c2} = 5.58$ K and $T_{c3} = 3.24$ K were obtained for magnetic field of $H = 1$ Oe. It should be noted that the onset of superconductivity at a temperature of $T_{c\ onset}$, which is close to 7 K is seen on the temperature dependences of *dc*-susceptibility in weak fields.

The degree of shielding of the external field in the nanocomposite below the superconducting transitions significantly differs (see Figures 1 and 2). For instance, only a very small fraction of the sample is shielded ($\sim 2 \cdot 10^{-5}$) in 1 Oe field after the first transition. Almost the entire sample is shielded after the second transition, and an additional

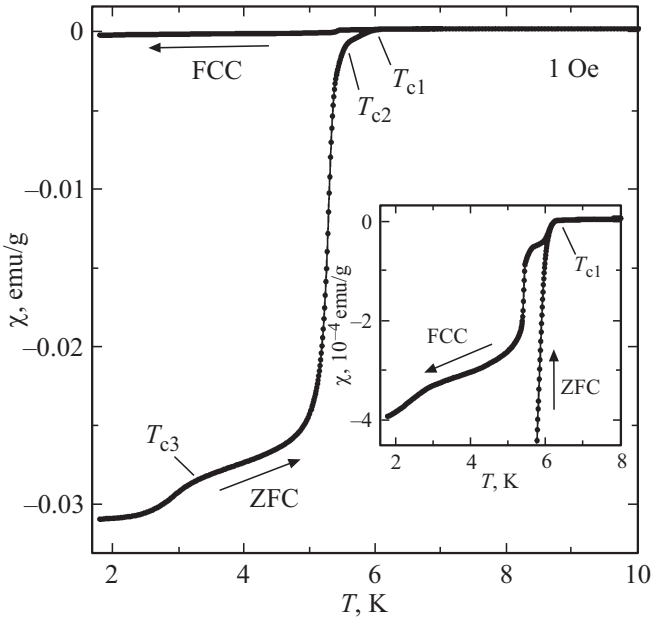

Figure 2. Temperature dependences of *dc*-susceptibility measured in ZFC and FCC modes in a magnetic field $H = 1$ Oe. The insert shows the area of the bifurcation of the ZFC and FCC curves.

shielding gain is observed after the third transition at a temperature of 1.8 K.

Figure 2 shows the temperature dependences of *dc*-susceptibilities obtained in the ZFC and FCC modes in 1 Oe field. It can be seen that the ZFC and FCC curves begin to diverge at temperatures below T_{c1}, however, a significant divergence occurs at temperatures below T_{c2}. ZFC susceptibility significantly differs from FCC susceptibility (by about 79 times) in the 1 Oe field and at a temperature of 1.8 K. This indicates the presence of strong pinning of superconducting vortices.

Figure 3 shows the field dependences of *dc*-magnetization at different temperatures. The irreversible behavior of $M(H)$ is observed at temperatures of 1.8, 3 and 4.5 K (Figure 3, *a*), which demonstrates strong pinning of superconducting vortices. The field dependence of the magnetization is partially reversible at a temperature of 6 K (Figure 3, *b*), which reflects the weak pinning of vortices.

Magnetic instabilities are observed in small magnetic fields on the $M(H)$ hysteresises at a temperature of 1.8 K and at sweeping rates of the magnetic field H above 50 Oe/sec which are manifested as sharp decreases of magnetization, followed by its gradual recovery (Figure 4). The number of „jumps“ of magnetization increases with an increase of the sweeping rate of the magnetic field. No magnetic instabilities were observed at temperatures of 3, 4.5 and 6 K.

Figure 5 shows a phase diagram in the field–temperature plane, constructed from the results of measurements of *dc*-magnetization for three superconducting transitions.

4. Discussion

Three superconducting transitions were found in this paper in a porous glass for a nanostructured Ga–In–Sn eutectic alloy at temperatures of $T_{c1} = 6.24$ K, $T_{c2} = 5.58$ K and $T_{c3} = 3.24$ K. At the same time, the beginning of the transition to a superconducting state was observed already at a temperature of $T_{c\,\mathrm{onset}} = 7$ K. T_{c2} and T_{c3} are close in values to the temperatures obtained in Ref. [11], based on measurements of magnetic ac magnetization for the same nanocomposite. The detection of anomalies

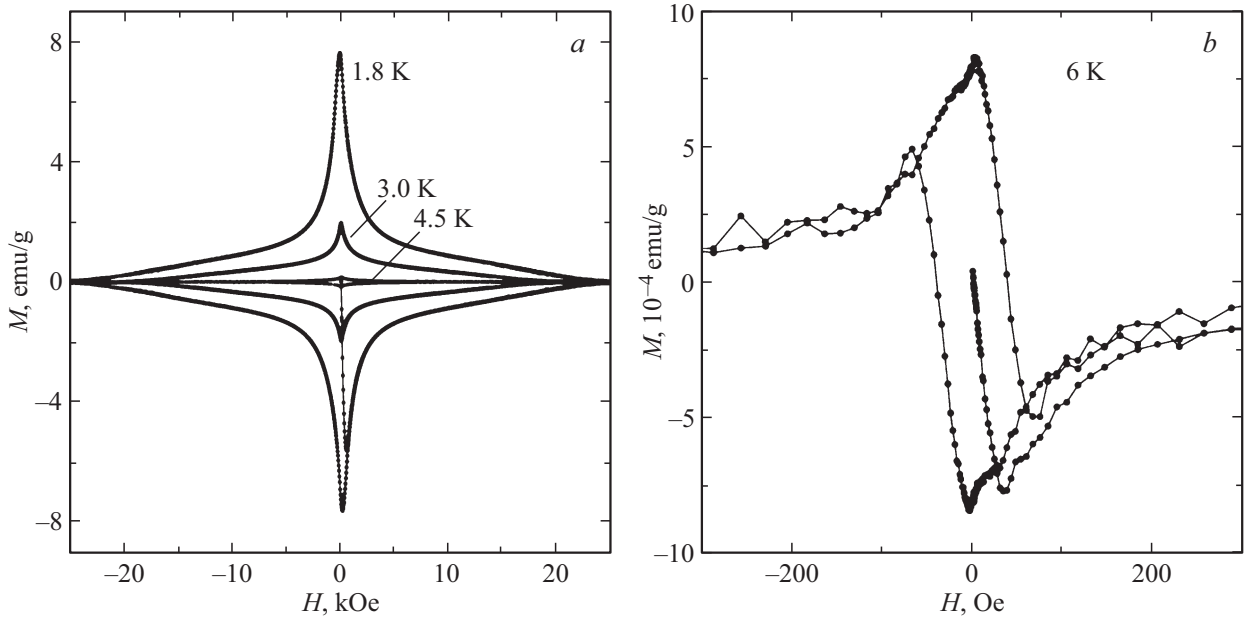

Figure 3. Isotherms of magnetization M at different temperatures, K: *a* — 1.8, 3 and 4.5; *b* — 6.

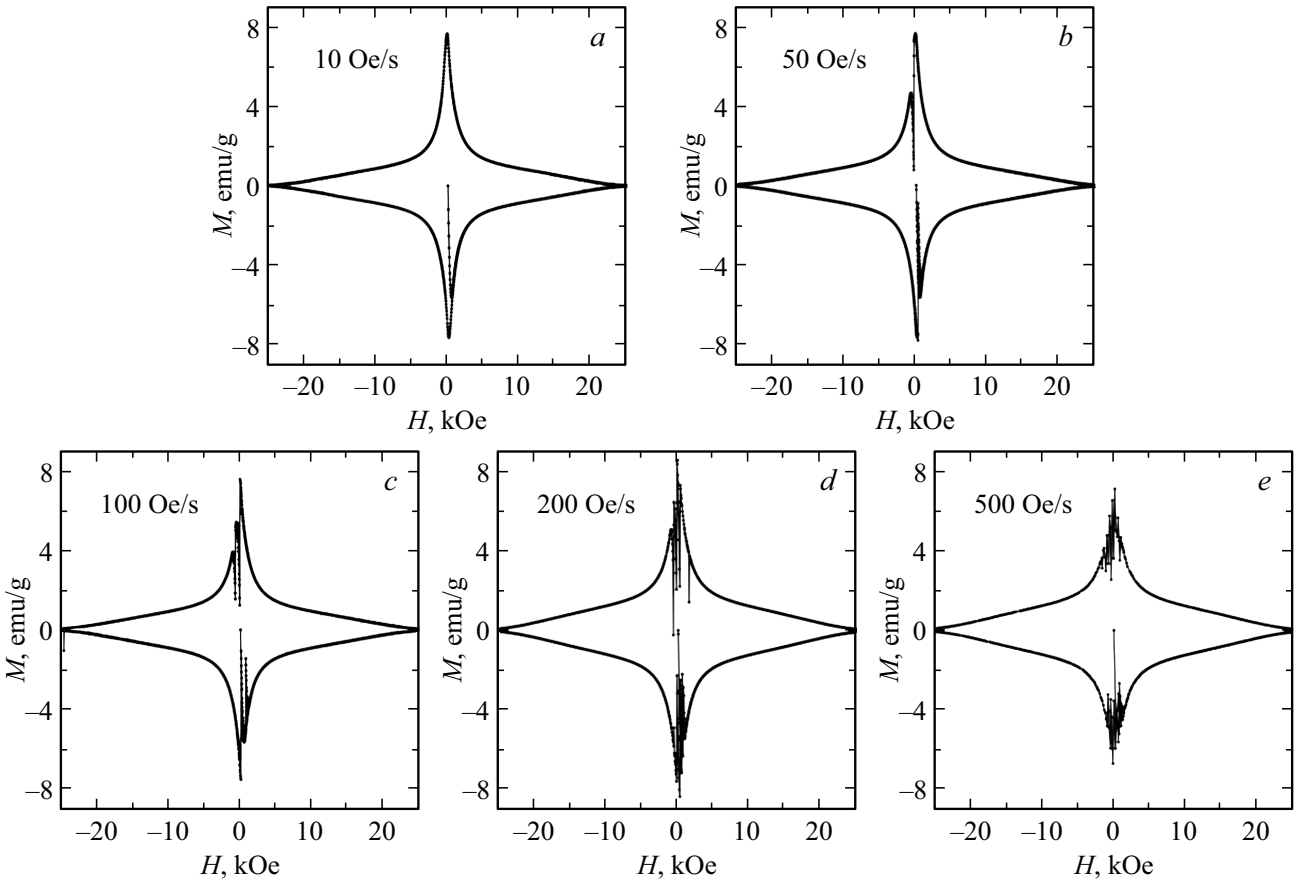

Figure 4. Isotherms of magnetization M at a temperature of 1.8 K for different sweeping rates of the magnetic field strength H.

of dc-susceptibility at temperatures $T_{c\,\mathrm{onset}}$ and T_{c1} can be explained by the higher sensitivity of the SQUID magnetometer compared to the complex PPMS-9 which was used for measuring ac-susceptibility in Ref. [11].

Study in Ref. [8] showed that segregates of gallium and intermetallic compounds of In_3Sn and $InSn_4$ are formed in case of crystallization from the melt in Ga–In–Sn bulk alloy having a composition close to the eutectic point. Intermetallic compounds of In_3Sn and $InSn_4$ were also found upon crystallization of the indium and tin alloy [13–16]. A superconducting transition with a critical temperature above 5 K [13] was observed in In–Sn bulk alloy in the region of the existence of In_3Sn intermetallic compound. Based on these data, it should be assumed that the superconducting transition discovered in this work in Ga–In–Sn nanostructured alloy at a temperature of $T_{c2} = 5.58$ K is attributable to the formation of segregates with the structure of In_3Sn. A similar conclusion was made in Ref. [11].

The superconducting transition with a critical temperature of $T_{c3} = 3.24$ K is obviously associated with the presence of indium segregates in the pores. The slight difference from the transition temperature for bulk indium (3.41 K) can be explained by size effects and the presence of small amounts of tin and gallium in indium segregates.

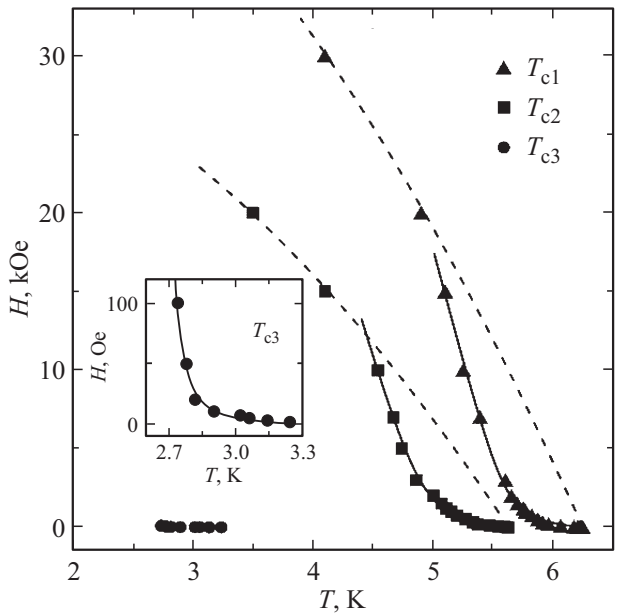

Figure 5. Phase diagram $H-T$. Dashed lines show fitting curves constructed using a two-fluid model using the formula (1), solid lines are calculated using a model that takes into account the proximity effect. The inset shows temperatures T_{c3} at an enlarged scale.

It should be noted that although indium was not found in Ref. [8] on the X-ray powder diffraction spectra of Ga–In–Sn bulk triple alloy, indium segregates can be formed in a nanostructured alloy due to the impact of nanoconfinement on the phase diagram.

The temperatures of the first superconducting transition T_{c1} and the onset of weak superconductivity $T_{c\,\mathrm{onset}}$ are much higher than the critical temperatures of bulk indium, gallium (1.08 K for α-gallium) and tin (3.73 K) [13,17]. However, it is known that gallium nanostructuring can result in the occurrence of crystalline phases other than α-Ga and having a superconducting transition at temperatures exceeding 6 K [18,19]. Thus, the occurrence of superconductivity at T_{c1} and $T_{c\,\mathrm{onset}}$ can presumably be associated with the polymorphism of gallium segregates.

The studied nanocomposite behaves like a dirty type-II superconductor, which is confirmed by the type of dependencies in Figures 2–4. The field dependence of magnetization is irreversible at temperatures of 1.8, 3 and 4.5 K (see Figure 3, *a*), which indicates the presence of strong pinning of vortices. The hysteresis is partially reversible at a temperature of 6 K (see Figure 3, *b*). It follows from this that at this temperature superconducting vortices are weakly fixed on pinning centers, this is confirmed by the temperature dependences of ZFC and FCC susceptibilities. Partially irreversible hysteresis has previously been observed in other superconducting nanocomposites [4,10,16,20].

The presence of magnetic instabilities on the field dependences of magnetization (see Figure 4) was previously experimentally observed in bulk and nanostructured superconductors [21–23]. According to theoretical concepts, the occurrence of such instabilities is associated with an avalanche-like redistribution of superconducting vortices caused by temperature fluctuations [22].

Temperature regions of positive curvature are observed for all critical lines in the phase diagram (Figure 5). The curvature becomes negative with the increase of the magnetic field for the first and second phase transitions. The negative curvature of the dependence of the upper critical field on temperature for type-II superconductors can be described in the framework of the two-fluid model [24]:

$$H_{c2}(T) = H_{c2}(0)\left(1 - \left(\frac{T}{T_{c0}}\right)^2\right), \qquad (1)$$

where $H_{c2}(0)$ is the upper critical field at zero temperature, T_{c0} is the temperature of the superconducting transition in the zero field. Approximation of critical lines in the region of large magnetic fields for the first and second superconducting transitions using the formula (1) gives the values of 53 and 32.5 kOe for the upper critical fields at zero temperature, respectively. These values are much higher than the upper critical field obtained for Ga–In–Sn bulk alloy [8]. The obtained values of the upper critical field make it possible to calculate the coherence length at zero temperature $\xi(0)$ based on Landau theory:

$$\xi(0) = \sqrt{\frac{\Phi_0}{2\pi H_{c2}(0)}}, \qquad (2)$$

where Φ_0 is the quantum flux.

The obtained coherence lengths for the first and second superconducting transitions (7.9 and 10.1 nm, respectively) are close to the pore diameter of the silicate matrix. This suggests that a decrease of the coherence length is associated with a limitation of the free path of electrons in nanoconfinement.

The positive curvature of the critical lines in the phase diagram was previously observed for many second-order superconductors of various kinds [2,4,11,20]. A theoretical model of a material representing a structure of alternating superconducting and non-superconducting layers connected by strong or weak Josephson links was proposed in Ref. [25] for the interpretation of positive curvature. Taking into account the proximity effect made it possible to describe the anomalous curvature of the critical lines. Solid lines in Figure 5 show the fitting curves obtained by the formula (13) from Ref. [25] for three transitions. The proximity effect ceases to play a significant role with an increase of the magnetic field.

5. Conclusion

The measurements of *dc*-magnetization for a nanocomposite based on a porous silicate matrix with a triple alloy of gallium, indium and tin introduced into the pores, the composition of which is close to the eutectic point, revealed a multistage character of the transition to a superconducting state. Three critical temperatures of 6.24, 5.58 and 3.24 K were determined in 1 Oe field. Weak superconductivity was observed below 7 K. Temperature and field dependences of dc magnetization show that the nanocomposite behaves like a dirty type-II superconductor. Superconducting transitions at 5.58 and 3.24 K are attributed to the formation of In_3Sn intermetallic compound and indium segregates in the nanostructured alloy, respectively. The transition at 6.24 K and weak superconductivity below 7 K are associated with the polymorphism of gallium segregates previously found for gallium in nanoconfinement. A positive curvature in small magnetic fields was observed in the constructed $H-T$ phase diagram on the critical lines for all three transitions, which was described using a model taking into account the proximity effect. Magnetic instabilities have been demonstrated on field dependences of magnetization at a temperature of 1.8 K.

Acknowledgments

The measurements were conducted using the equipment of the St. Petersburg State University Research Park.

Funding

This study was supported financially by grant No. 21-72-20038 from the Russian Science Foundation.

Conflict of interest

The authors declare that they have no conflict of interest.

References

[1] R. Wördenweber, V. Moshchalkov, S. Bending, F. Tafuri. Superconductors at the Nanoscale. From Basic Research to Applications. De Gruyter, Berlin (2017). 494 p.
[2] E.V. Shevchenko, E.V. Charnaya, M.K. Lee, L.-J. Chang, M.V. Likholetova, I.E. Lezova, Y.A. Kumzerov, A.V. Fokin. Physica C **574**, 1353666 (2020).
[3] S. Bose. Supercond. Sci. Technol **36**, *6*, 063003 (2023).
[4] E.V. Charnaya, C. Tien, K.J. Lin, C.S. Wur, Y.A. Kumzerov. Phys. Rev. B **58**, *1*, 467 (1998).
[5] N. Ochirkhuyag, R. Matsuda, Z. Song, F. Nakamura, T. Endo, H. Ota. Nanoscale **13**, *4*, 2113 (2021).
[6] P.S. Banerjee, D.K. Rana, S.S. Banerjee. Adv. Colloid Interface Sci. **308**, 102752 (2022).
[7] Z. Yao, M. Sandberg, D.W. Abraham, D.J. Bishop. Appl. Phys. Lett. **124**, *26*, 264002 (2024).
[8] T. Mochiku, M. Tachiki, S. Ooi, Y. Matsushita. Physica C **563**, 33 (2019).
[9] L. Ren, J. Zhuang, G. Casillas, H. Feng, Y. Liu, X. Xu, Y. Liu, J. Chen, Y. Du, L. Jiang, S.X. Dou. Adv. Func. Mater. **26**, *44*, 8111 (2016).
[10] T.-T. Zhang, G.-X. Xie, G.-T. Cheng, S.-H. Chen, D.-Y. Zhu, Y.-R. Zhang, W.-P. Han, D. Chen, Y.-Z. Long. J. Mater. Sci.: Mater. Electron. **33**, *13*, 1 (2022).
[11] O.D. Shevtsova, M.V. Likholetova, E.V. Charnaya, E.V. Shevchenko, Yu.A. Kumzerov, A.V. Fokin. FTT **64**, *1*, 40 (2022). (in Russian).
[12] Y. Plevachuk, V. Sklyarchuk, S. Eckert, G. Gerbeth, R. Novakovic. J. Chem. Eng. Data **59**, *3*, 757 (2014).
[13] M.F. Merriam, M. Von Herzeni. Phys. Rev. **131**, *1*, 637 (1963).
[14] R. Kubiak, M. Wołcyrz, W. Zacharko. J. Less-Common Met. **65**, *2*, 263 (1979).
[15] Y. Shu, T. Ando, Q. Yin, G. Zhou, Z. Gu. Nanoscale **9**, *34*, 12398 (2017).
[16] A.S. Gandhi, P.-H. Shih, S.Y. Wu. Supercond. Sci. Technol. **25**, *6*, 105006 (2012).
[17] G. Knapp, M.F. Merriam. Phys. Rev. **140**, *2A*, 528 (1965).
[18] E.V. Charnaya, C. Tien, M.K. Lee, Y.A. Kumzerov. J. Phys. Condens. Matter **21**, *45*, 455304 (2009).
[19] R.D. Heyding, W. Keeney, S.L. Segel. Phys. Chem. Solids J. **34**, *1*, 133 (1973).
[20] D.V. Smetanin, M.V. Likholetova, E.V. Charnaya, M.K. Lee, L.J. Chang, E.V. Shevchenko, Yu.A. Kumzerov, A.V. Fokin. Phys. Solid State **64**, *8*, 942 (2022).
[21] R.G. Mints, A.L. Rakhmanov, Rev. Mod. Phys. **53**, *3*, 551 (1981).
[22] C. Tien, A.L. Pirozerskii, E.V. Charnaya, D.Y. Xing, Y.S. Ciou, M.K. Lee, Y.A. Kumzerov. J. Appl. Phys. **109**, *5*, 053905 (2011).
[23] A. Gerber, J.N. Li, Z. Tarnawski, J.J.M. Franse, A.A. Menovsky. Phys. Rev. B **47**, *10*, 6047 (1993).
[24] M. Tinkham Introduction to Superconductivity. 2nd. ed. Dover Publications (2004).
[25] S. Theodorakis, Z. Tešanovic. Phys. Rev. B **40**, *10*, 6659 (1989).

Translated by A.Akhtyamov